Integrative analysis of miRNA and mRNA paired expression profiling of primary fibroblast derived from diabetic foot ulcers reveals multiple impaired cellular functions

Liang Liang, PhD[1]; Rivka C. Stone, MD, PhD[1]; Olivera Stojadinovic, PhD[1,2]; Horacio Ramirez, PhD[1,3]; Irena Pastar, PhD[1]; Anna G. Maione, PhD[4,5]; Avi Smith, BA[6]; Vanessa Yanez, MA[6]; Aristides Veves, MD, DSc[7]; Robert S. Kirsner, MD[1,2]; Jonathan A. Garlick, PhD, DDS[4,5]; Marjana Tomic-Canic, PhD[1,2,3,6]

1. Department of Dermatology & Cutaneous Surgery, University of Miami Miller School of Medicine (UMMSOM), Wound Healing and Regenerative Medicine Research Program,
2. Wound Healing Clinical Research Program, UM Health System, Miami, Florida,
3. Human Genomics and Genetics Graduate Program,
4. Department of Cell, Molecular, and Developmental Biology, Sackler School of Graduate Biomedical Sciences, Tufts University,
5. Department of Oral and Maxillofacial Pathology, School of Dentistry, School of Medicine, School of Engineering, Tufts University, Boston, Massachusetts,
6. John P. Hussman Institute for Human Genomics, University of Miami Miller School of Medicine (UMMSOM), Miami, Florida,
7. Beth Israel Deaconess Medical Center, Boston, Massachusetts

Reprint requests:
Marjana Tomic-Canic, PhD, Department of Dermatology and Cutaneous Surgery, University of Miami Miller School of Medicine, 1600 NW 10th Avenue, RMSB, Room 2023-A, Miami, FL 33136, USA.
Tel: 305-243-4940;
Fax: 305-243-6191;
Email: mtcanic@med.miami.edu

Manuscript received: April 11, 2016
Accepted in final form: August 20, 2016

DOI:10.1111/wrr.12470

ABSTRACT

Diabetic foot ulcers (DFUs) are one of the major complications of diabetes. Its molecular pathology remains poorly understood, impeding the development of effective treatments. Although it has been established that multiple cell types, including fibroblasts, keratinocytes, macrophages, and endothelial cells, all contribute to inhibition of healing, less is known regarding contributions of individual cell type. Thus, we generated primary fibroblasts from nonhealing DFUs and evaluated their cellular and molecular properties in comparison to nondiabetic foot fibroblasts (NFFs). Specifically, we analyzed both micro-RNA and mRNA expression profiles of primary DFU fibroblasts. Paired genomic analyses identified a total of 331 reciprocal miRNA–mRNA pairs including 21 miRNAs ($FC > 2.0$) along with 239 predicted target genes ($FC > 1.5$) that are significantly and differentially expressed. Of these, we focused on three miRNAs (miR-21-5p, miR-34a-5p, miR-145-5p) that were induced in DFU fibroblasts as most differentially regulated. The involvement of these microRNAs in wound healing was investigated by testing the expression of their downstream targets as well as by quantifying cellular behaviors in prospectively collected and generated cell lines from 15 patients (seven DFUF and eight NFF samples). We found large number of downstream targets of miR-21-5p, miR-34a-5p, miR-145-5p to be coordinately regulated in mRNA profiles, which was confirmed by quantitative real-time PCR. Pathway analysis on paired miRNA–mRNA profiles predicted inhibition of cell movement and cell proliferation, as well as activation of cell differentiation and senescence in DFU fibroblasts, which was confirmed by cellular assays. We concluded that induction of miR-21-5p, miR-34a-5p, miR-145-5p in DFU dermal fibroblasts plays an important role in impairing multiple cellular functions, thus contributing to overall inhibition of healing in DFUs.

Wound healing is a dynamic cellular response to cutaneous injury, which requires temporal and spatial regulation of multiple cell types. However, deregulation of wound healing-specific cellular processes is a major contributor of inhibited healing in patients with DFUs. DFUs represent a major clinical challenge in the current healthcare system.[1] It has been established that over 100 known physiologic factors are involved in the inhibition of wound healing of DFUs.[2,3] Thus, understanding pathophysiology of individual cell type and its implications to cellular functions in tissue samples from DFU patients may hold a key to understanding inhibition of healing in DFUs.

Fibroblasts are the major cellular component of dermis. They play important role in many essential aspects of the repair processes, including regulation of angiogenesis, collagen depositions, quantity of granulation tissue, as well as production and remodeling of extracellular matrix (ECM), all of which are found to be dysregulated in DFUs.[4] Nevertheless, the molecular pathophysiology and in-depth phenotypic characterization of DFU fibroblasts remains unexplored.

We and others have shown previously that primary dermal fibroblasts can be successfully cultured from patients' biopsies obtained from venous leg ulcers (VLUs) and DFUs.[5–7]

More importantly, we have demonstrated recently that primary fibroblasts generated from DFUs not only maintain DFU pathogenic phenotype in culture but can also cross-talk to healthy keratinocytes in three-dimensional (3D) organotypic cultures, conveying pathogenic signals to healthy "partner" cells.[6] To further understand molecular makeup of DFU fibroblasts. We used patients' tissue samples to generate primary cell lines and utilized genomic approaches to analyze differential expression of miRNAs and mRNAs. miRNAs are small noncoding RNAs that regulate posttranscriptional gene expression by binding to the 3′ UTR of mRNAs, resulting in repression of mRNA translation or degradation.[8] As a class of fine-tuning regulators, miRNAs have been shown to regulate various pathogenic processes of skin diseases, such as psoriasis and hypertrophic scarring.[9,10] Our lab and others have shown that aberrant expression of miRNAs can contribute to inhibition of healing in chronic wounds. In particular, up-regulation of miR-16, miR-20a, miR-21, miR-106a, miR-130a, and miR-203 were found in nonmigratory epidermis of VLUs.[11] In addition, miR-21 and miR-130a inhibited epithelialization in vivo and ex vivo by directly targeting EGR3 and LepR.[11] In an ischemic murine wound model, hypoxia-induced miR-203 and miR-210 expression were found to inhibit wound closure and keratinocyte proliferation.[12] However, the functional role of miRNAs in fibroblasts derived from DFU tissue have not been previously investigated.

In this study, we utilized an integrative approach, by combining genome-wide mRNA and miRNA array analysis of DFU-derived fibroblast (DFUF), miRNA target predictions, miRNA–mRNA expression pairings and pathway analysis to identify pathogenic pathways regulated by specific miRNAs. Utilizing primary fibroblast cell lines generated from DFUs (DFUFs) and nondiabetic foot fibroblasts (NFFs) as controls, we identified three miRNAs (miR-34a-5p, miR-21-5p, and miR-145-5p) as up-regulated along with their 13 predicted down-regulated target genes. The following cellular functions: proliferation, migration, differentiation, and senescence were evaluated in comparison of DFUFs to NFFs. Taken together, we conclude that altered miRNA–mRNA expression in DFUFs contributes to delayed cell proliferation and migration, as well as induced differentiation and cell senescence, suggesting that dysregulation of aforementioned miRNAs may play a significant role in DFUs fibroblast function and subsequently inhibition of wound healing.

MATERIALS AND METHODS

Primary fibroblasts cell culture

Foot skin specimens were obtained under the IRB approved protocol IRB# 20120574. Diabetic foot ulcer fibroblasts (DFUF) were generated from tissue samples obtained at the site of wound edge of diabetic patients with a nonhealing DFU, and NFF from healthy, nondiabetic donors. Patient demographics and details of isolation of primary fibroblasts from skin specimens was previously described.[6,13] Primary fibroblasts were maintained in fibroblast growth media containing DMEM (1 g/L glucose) (Invitrogen, Carlsbad, CA), 10% fetal bovine serum (HyClone, Logan, UT), HEPES (Sigma-Aldrich, St. Louis, MO), and Pen/Strep/Fung (Invitrogen) at 37 °C. Cells were passaged when confluent using 0.05% trypsin/EDTA (Invitrogen) and all experiments were conducted on passages 4–7.

RNA extraction, micro-RNA, and mRNA gene expression arrays

Primary fibroblasts at passage 4 were grown until confluence and total RNA with miRNA fraction was isolated using miRNeasy Mini kit (Qiagen, Hilden, Germany) per manufacturer's instructions. RNA quality and purity was examined using nanodrop (Thermo Scientific, Waltham, MA) and bioanalyzer (Agilent, Santa Clara, CA). Samples with an RNA Integrity Number (RIN) of 8 or greater were used.

Eight primary fibroblast cell lines (NFFs ($n = 4$) and DFUFs ($n = 4$)), were used to generate miRNA and mRNA gene expression profiles. NanoString nCounter microRNA expression assay v2 panel (NanoString, Seattle, WA) containing 800 mature microRNA probes was used to analyze microRNA expression profiles. Genome-wide transcriptional expression was analyzed using Illumina HumanHT-12 v4 Expression BeadChip array containing more than 47,000 probes (Illumina, San Diego, CA). Both miRNA and mRNA expression raw data was analyzed using GeneSpring GX (Agilent, Japan). The differentially expressed transcripts were considered to be miRNAs with $p < 0.05$ and fold changes ≥ 2.0, and mRNAs with $p < 0.05$ and fold changes ≥ 1.5. MiRNA–mRNA expression paring analysis and pathway analysis was performed using online software Ingenuity Pathway Analysis (IPA) (Qiagen, Redwood City, CA). Nanostring miRNA profiles are publically available in GEO database under the super series GSE84971.

MicroRNA quantitative real-time PCR and gene expression analysis

To provide more power for integration of genomic with quantitative real-time PCR (qPCR) data, additional NFFs ($n = 5$) and DFUFs ($n = 4$) were prospectively generated and included in validation of miRNA and mRNA expressions. qScript microRNA Quantification System (Quanta BioSciences, Inc., Gaithersburg, MD) was used to assess microRNA expression. Briefly, cDNA was synthesized from total RNA including the microRNA fraction using the qScript microRNA cDNA Synthesis Kit (Quanta BioSciences, Inc.). 1 ng of cDNA per PCR reaction was used with a CFX Connect™ Real-Time PCR Detection System (Bio-Rad). Small nucleolar RNA C/D box 48 (SNORD48) was used as a reference gene to calculate miRNA relative expression.

For gene expression analysis, cDNA was made using qScript cDNA Synthesis kit (Quanta BioSciences, Inc.) and actin related protein 2/3 complex, subunit 2 (ARPC2) was used as a reference gene. All real-time PCR reactions were done in triplicate using PerfeCTa SYBR Green SuperMix (Quanta BioSciences, Inc.). Relative gene expression was calculated using the ddCT method. Sequence of primers used in qPCR are presented in Table 1.

Table 1. Primer sequences of targets genes

Gene Symbol		Sequence(5′-3′)
ABCA1	Forward primer	TTCCCGCATTATCTGGAAAGC
	Reverse primer	CAAGGTCCATTTCTTGGCTGT
CD47	Forward primer	AGAAGGTGAAACGATCATCGAGC
	Reverse primer	CTCATCCATACCACCGGATCT
GAS1	Forward primer	ATGCCGCACCGTCATTGAG
	Reverse primer	TCATCGTAGTAGTCGTCCAGG
GLIS3	Forward primer	AGAATGGCCTTGATCTAGGGG
	Reverse primer	GTGCCAAAAAGGTAGGATGGTAA
IRS1	Forward primer	CCCAGGACCCGCATTCAAA
	Reverse primer	GGCGGTAGATACCAATCAGGT
PDGFD	Forward primer	TTGTACCGAAGAGATGAGACCA
	Reverse primer	GCTGTATCCGTGTATTCTCCTGA
PDGFRA	Forward primer	TTGAAGGCAGGCACATTTACA
	Reverse primer	GCGACAAGGTATAATGGCAGAAT
PTGFR	Forward primer	GAGCGGTGTATTGGAGTCACA
	Reverse primer	GTCCTCGACGCCTGAATTTTA
RECK	Forward primer	TGTGAACTGGCTATTGCCTTG
	Reverse primer	GCATAACTGCAACAAACCGAG
S100A10	Forward primer	GGCTACTTAACAAAGGAGGACC
	Reverse primer	GAGGCCCGCAATTAGGGAAA
SPRY1	Forward primer	TCCCTGGTCATAGGTCTGAAAG
	Reverse primer	TGCCGGTTACAGGCCAAAC
STAT3	Forward primer	CAGCAGCTTGACACACGGTA
	Reverse primer	AAACACCAAAGTGGCATGTGA

MTT cell proliferation assay

Cell proliferation was measured by using colorimetric MTT (3-(4,5-dimethylthiazol-2-yl)−2,5-diphenyl tetrazolium bromide) assay (Sigma-Aldrich). In brief, primary fibroblasts at passage 6 were seeded at 10×10^3 cells/well in 24-well plate. On day 4 after seeding (~80% confluence), cells were incubated with 5 mg/mL MTT solution for 4 h at 37 °C. Then MTT solution was aspirated, and the formazan product was solubilized with dimethyl sulfoxide. Cell proliferation was assessed by measuring the absorbance at 570 nm. Background absorbance was corrected by subtracting readings at 690 nm.

Scratch assay

Primary fibroblasts at passage 6 were grown in 24-well plates and fibroblast medium was then replaced with DMEM containing 30 mM glucose for 48 h. Scratches were performed using a 200-μL pipette tip. Cell migration were recorded by photographing immediately at 0, 4, and 8 h after monolayer scratch with an inverted microscope. Migration distance was measured using ImageJ software. 20–25 measurements were taken for each cell line. Rate of cell migration was expressed as a percent of distance coverage by cells moving into the scratched area for each time point after wounding. Representative microscopic images are shown.

Western blot

Protein samples were collected from DFUFs and NFFs ($n = 6$) at passage 1–3. Protein extraction and Western blot was performed as described previously.[14] Antibodies used in this study included anti-caspase 1(1:1,000; Cell Signaling), -caspase 3 (1:1,000; Cell Signaling), -α-smooth muscle actin (1:1,000; Sigma), and GAPDH (1:2,000; Santa Cruz) as loading control.

Senescence associated β-galactosidase staining

Staining for SA-β gal was performed by using a commercial β-galactosidase staining kit (Cell Signaling Technology, Danvers, MA) as per manufacturer's instructions. All the experiments were done in triplicates using passage 7 fibroblasts. Representative microscopic images are shown in Figure 4.

Immunocytochemistry

Fibroblasts were cultured until reaching confluence and fixed with 4% paraformaldehyde for 10 min. Cells were blocked in 5% BSA in PBS for 1 h. Mouse monoclonal antibodies detecting α-smooth muscle actin (α-SMA) (Sigma) were diluted to 1:10,000 in 5% BSA and incubated overnight at 4 °C. Signal was visualized using Alexa Fluor 594 (Invitrogen, Carlsbad, CA) secondary antibodies, and slides were mounted with mounting medium containing

DAPI to visualize nuclei (Life Technology). Nikon Eclipse E800 microscope was used for visualization, and digital images were collected using SPOT Camera Advanced program (Nikon, Melville, NY).

Statistics

Results are presented as mean ± SEM of at least three independent specimens. Statistical analyses were performed using Prism (Graphpad Software, La Jolla, CA). For miRNA and gene expression data, statistical significance was determined by two-tailed Mann-Whitney test. For *in vitro* cellular functional assays, statistical significance was determined by two-tailed unpaired student *t*-test. Level of significance were set at $p < 0.05$. $*p < 0.05$, $**p < 0.001$, $***p < 0.0001$.

RESULTS

Microarray analysis reveals differentially expressed miRNAs and correlated downstream mRNA targets in primary DFUF

To identify miRNAs differentially expressed in DFUFs that may delay wound healing, we compared both miRNA and mRNA profiles of DFUF and NFF cell lines. In previous studies, the same fibroblast cell lines have been characterized in the perspectives of global DNA methylation,[7] and in 3D tissue models,[6] in which DFUFs demonstrated to maintain diabetic ulcer phenotypes by stimulating hyper-proliferation of keratinocytes, showing reduced stimulation of angiogenesis, reepithelialization, and producing impaired ECM.[6] In this particular study, we focused on the investigation of intrinsic cellular functions of DFU-derived primary fibroblasts in comparison to those derived from healthy nondiabetic foot skin.

Unsupervised hierarchical clustering of both miRNA and mRNA expression analysis grouped four DFUFs and four NFFs into two distinct branches, except for one cell line of each (NFF11 and DFU7) (Figure S1A). Further analysis in miRNA and mRNA expression similarity test identified the same cells lines (NFF11 and DFU7) which did not present similar patterns compared to the rest cell lines within the same group (Figure S1B). Therefore, we consider NFF11 and DFU7 as outliers, perhaps as a result of individual patient variabilities, and were excluded from subsequent microarray analysis.

On comparative analyses among three DFUF and three NFF cell lines, we found a total of 21 miRNAs differentially expressed with $p < 0.05$ and fold change ≥ 2.0. Of these, 11 miRNAs were up-regulated and 10 miRNAs were down-regulated in DFUFs (Figure 1A). Next, we incorporated differentially expressed mRNA transcripts into miRNA profiles by preforming miRNA–mRNA expression pairing analysis using IPA software. In brief, a subset of genes from the complete differential expression profiles of DFUFs were selected when genes meet both of the following requirements: (1) predicted as targets of differentially expressed miRNAs; (2) expression in the opposite direction of their targeting miRNAs (miRNA up/mRNA down, or miRNA down/mRNA up). The prediction for miRNA targets was either experimentally observed or had a high or moderate prediction score calculated by IPA. Utilizing this approach we selected the specific subset of mRNAs that were primarily regulated by 21 differentially expressed miRNAs identified in the same pool of DFUFs. With the criteria of $p < 0.05$ and fold change ≥ 1.5 for the differentially expressed mRNAs, we found 239 differentially expressed target genes and 331 reciprocal miRNA–mRNA pairs in DFUFs vs. NFFs. Paring differentially regulated mRNAs with miRNAs allowed us to extract specific functional pathways that are predominantly regulated by miRNAs identified in DFUF profiles.

miRNA regulatory networks predict impaired cellular functions

Next, we focused on the abundantly expressed miRNAs that showed the largest difference in fold change (miR-21-5p, -34a-5p, -143-3p, -145-5p) between DFUFs and NFFs, and constructed functional regulatory network with their paired target genes (Figure S2). Of the 16 miRNA–mRNA parings that we focused in this study (Figure 1B), 4 pairings have been experimentally validated, including miR-21-5p/RECK, SPRY1, miR-34a-5p/CD47, miR-145-5p/IRS1[15–19]; whereas 12 pairings namely, miR-21-5p/CD47, S100A10, STAT3, miR-34a-5p/GAS1, RECK, IRS1, PDGFRA, miR-145-5p/ABCA1, GLIS3, PDGFD, PTGFR, miR-143-3p/PDGFRA are novel and, to the best of our knowledge, have not been previously described. Interestingly, four genes (CD47, RECK, IRS1, and PDGFRA) are downstream targets of multiple miRNAs, indicating synergistic relationships of these up-regulated miRNAs. Furthermore, regulatory network mediated by these dysregulated miRNAs predicts diverse effects on the following cellular functions, including inhibitions of cell movement and proliferation, activation of cell differentiation and senescence (Figure 1B).

qPCR validates expression of miRNAs and their target mRNAs

To validate miRNAs expression data, we performed miRNA qPCR using a larger set of additional cell lines generated from prospectively collected tissue samples, DFUF ($n = 7$) and NFF ($n = 8$). qPCR shows an induction of miR-21-5p in DFUFs by 1.6-fold ($p = 0.029$), miR-34a-5p by 2.5-fold ($p = 0.0001$), and miR-145-5p by 2.2-fold ($p = 0.04$) (Figure 2A). Due to patient variability, induction in miR-143-3p (1.9-fold) in DFUFs did not reach statistical significance ($p = 0.3$). However, we found a significant correlation between the expression of miR-143-3p and miR-145-5p ($r = 0.92$, $p < 0.00001$) (Figure 2B). In fact, encoding genes of miR-143 and miR-145 are located in close proximity on human chromosome 5 and are considered to be co-transcribed in the same bicistronic transcript.[20] Cluster of miR-143/-145 are abundantly expressed specifically in fibroblasts and smooth muscle cells as oppose to epithelial and endothelial cells in colon.[21] Thus, miRNA qPCR data using a larger scale of samples are in agreement with miRNA microarray analysis.

Next, we performed qPCR of mRNA to examine target gene expressions using the same cohort of primary fibroblasts. Consistent with mRNA microarray analysis, 12 target genes involved in impaired cellular functions were

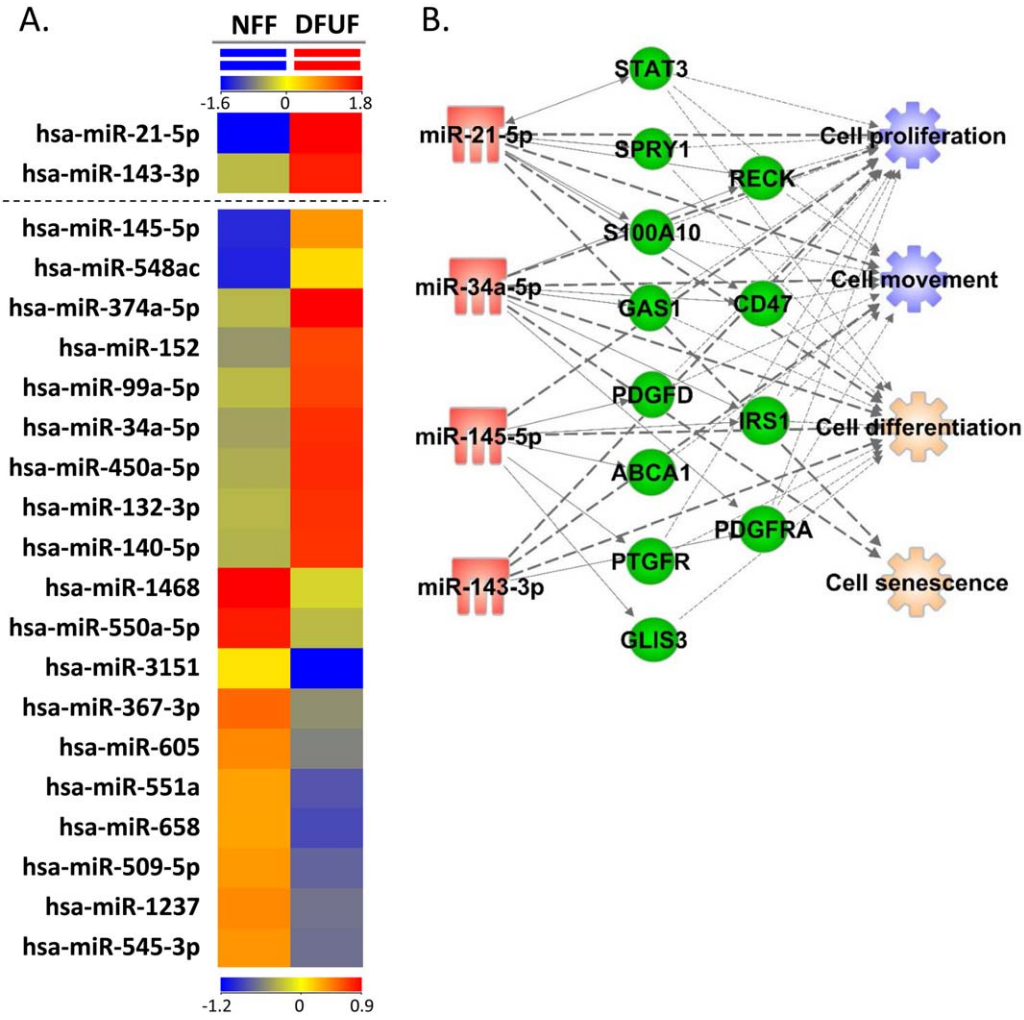

Figure 1. Diabetic foot ulcer fibroblasts (DFUFs) miRNA profiles reveal differentially expressed miRNAs as compared to normal foot fibroblasts (NFFs). (A) Heat maps demonstrating normalized miRNA expression levels in DFUFs and NFFs. Differentially regulated miRNAs ($n = 21$) are identified by student t-test ($p < 0.05$) with a fold change greater than 2.0. (B) Predicted regulatory effects in signaling pathways based on the expressions of paired miRNAs (FC > 2.0) and mRNAs (FC > 1.5) identified from DFUF profiles ($p < 0.05$). Network was constructed by IPA. Red and green colors indicate up- and down-regulated miRNAs/genes, respectively. Orange and blue colors indicate predicted activation and inhibition, respectively.

significantly down-regulated in DFUFs compared to NFFs ($p < 0.05$), namely ABCA1 (9.7-fold), CD47 (1.4-fold), GAS1 (7.1-fold), GLIS3 (7.6-fold), IRS1 (2.7-fold), PDGFD (21.5-fold), PDGFRA (17-fold), PTGFR (16.6-fold), RECK (14.7-fold), S100A10 (13.3-fold), SPRY1 (7.2-fold), STAT3 (5.8-fold) (Figure 2C). Therefore, we confirmed the induction of miR-21-5p, miR-34a-5p, miR-145-5p, and 12 of their repressed downstream targets in DFUFs, further supporting microarray profiling.

DFUFs exhibit delayed cell proliferation, cell migration, and enriched in myofibroblasts

To investigate miRNA-regulated cellular functions based on DFUF miRNA–mRNA profiles, we performed MTT assay, scratch assay, and western blot to evaluate cell proliferation and migration in DFUFs and compared them to NFFs (Figure 3A–C). We found a statistically significant decrease in cell proliferation of DFUFs compared to NFFs by day 4 after seeding ($p = 0.036$) (Figure 3A). Meanwhile, DFUFs migrated slower than NFFs at 4 and 8 h after wounding ($p < 0.05$) (Figure 3B and C). Taken together, we conclude that functional cellular assessments confirmed inhibition of cell proliferation and migration in DFUFs as predicted by miRNA regulated regulatory networks.

According to IPA analyses (Figure 1B), all four miRNAs (miR-21-5p, −34a-5p, −143-3p, −145-5p) are involved in activated cell differentiation. Hence, we utilized antibodies against a myofibroblast marker, α-smooth

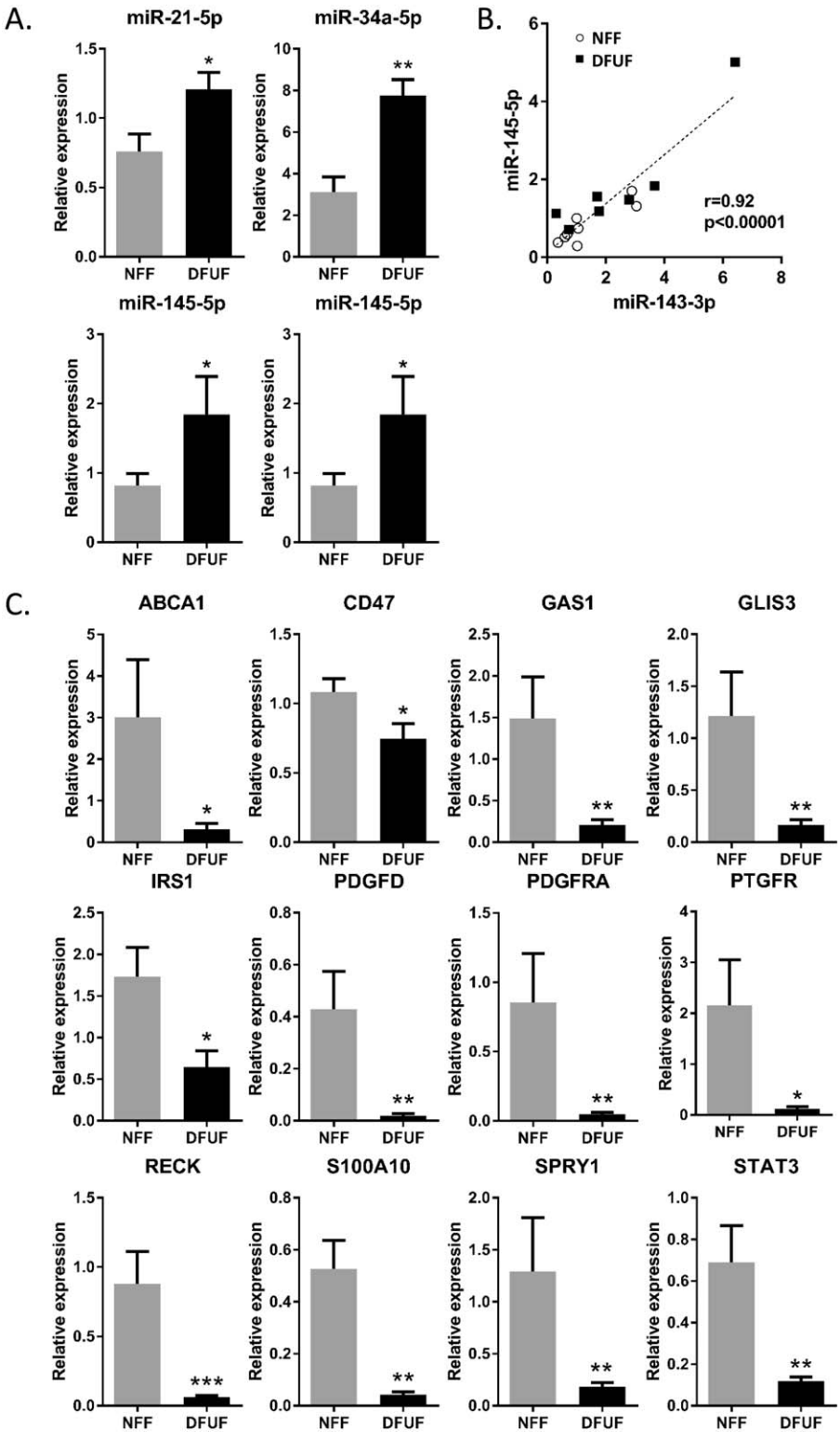

Figure 2. qPCR validation of differentially regulated miRNAs and target genes. (A) qPCR validation of differentially expressed miRNAs in DFUFs vs. NFFs. (B) Positive correlations between miR-145-5p and miR-143-3p. (C) qPCR validation of differentially expressed mRNAs in DFUFs vs. NFFs. Plots represent the averaged relative expression levels of mRNA of DFUFs ($n = 7$) samples and NFFs ($n = 8$) samples. $^{*}p < 0.05$, $^{**}p < 0.001$, $^{***}p < 0.0001$.

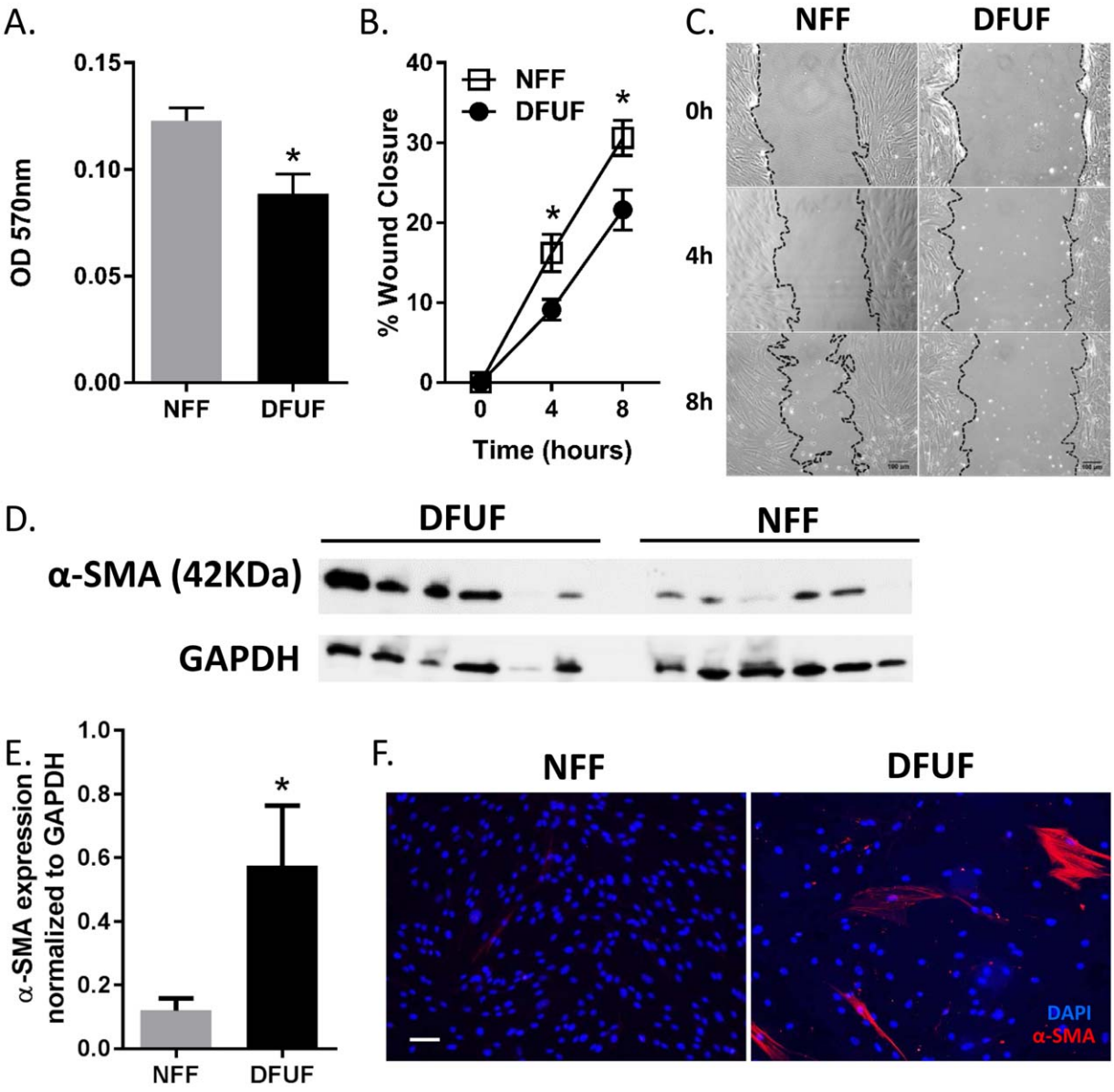

Figure 3. Cell proliferation and cell migration are delayed and myofibroblasts are enriched in DFUFs compared to NFFs. (A) Quantifications of MTT cell proliferation assay and (B) scratch wound assay for DFUFs ($n = 3$) and NFFs ($n = 3$). (C) Representative phase contrast microscopic images of scratch wounds of DFUFs and NFFs at 0, 4, and 8 hours. (D) Western blot and (E) quantifications of α-SMA in DFUFs and NFFs ($n = 6$). (F) Representative immunofluorescence images of α-SMA staining. Results are expressed as mean ± S.E.M of each group of fibroblasts. $^*p < 0.05$. Scale bar 100 μm.

muscle actin (α-SMA), to evaluate cell differentiation in fibroblasts (Figure 3D–F). We identified a 4.8-fold induction of α-SMA expression in DFUFs ($p = 0.039$) by western blot (Figure 3D and E), and an increased number of α-SMA+ cells by immunofluorescent staining (Figure 3F). These observations once again confirmed the predictions generated by miRNA regulatory networks, suggesting myofibroblasts are not only present in DFUF primary cell cultures but are also statistically significantly increased when compared to NFFs.

DFUFs show induced cell senescence

Another activated cellular function predicted by IPA analysis is cell senescence (Figure 1B). Out of 50 genes previously identified from replicative senescent fibroblasts,[22] we found 12 genes regulated to the same directions (DFUFs vs NFFs, *t*-test, $p < 0.05$) (Figure 4A). To functionally validate genomics findings we examined cell senescence in DFUFs, using senescence associated β-galactosidase staining (Figure 4B and C). We stained

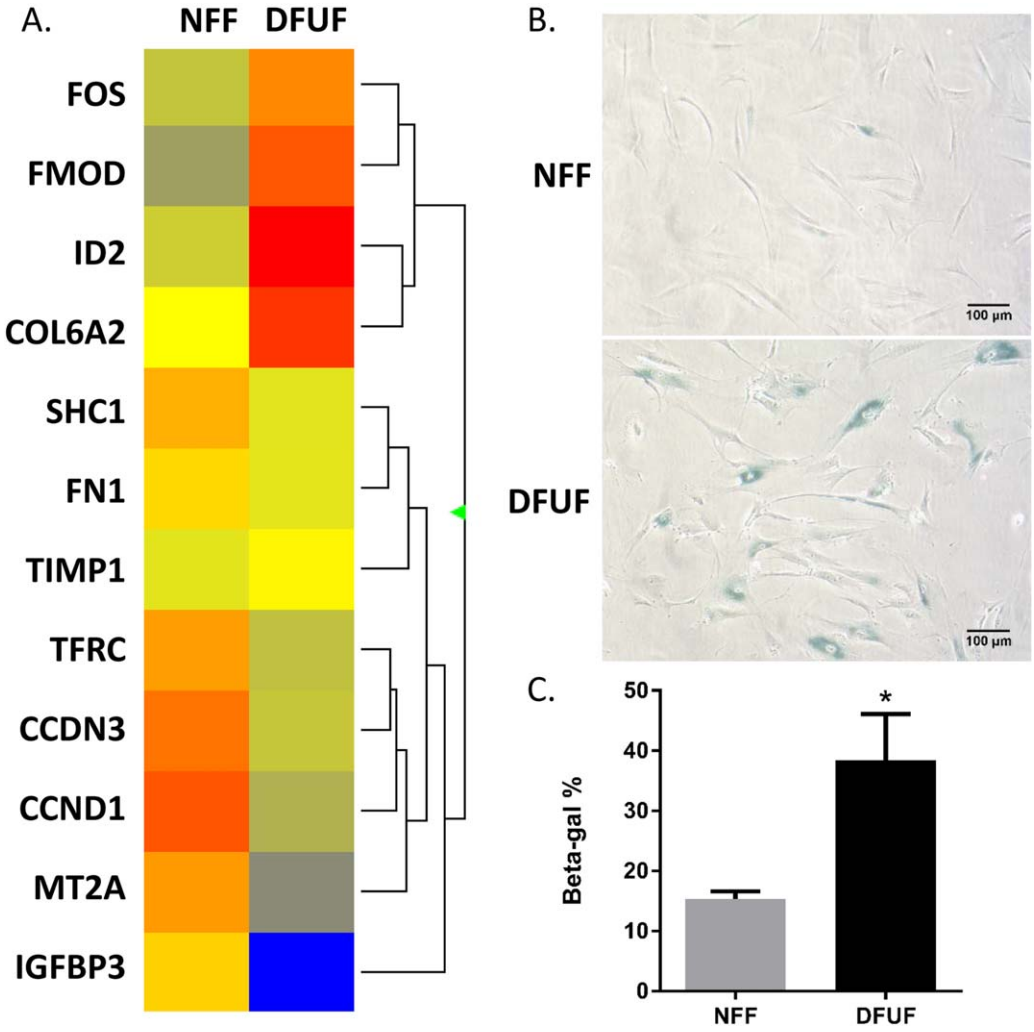

Figure 4. Cell senescence is induced in DFUFs compared to NFFs. (A) 12 differentially regulated genes previously reported[20] in senescent fibroblasts are identified from DFUF profiles. (B) Representative phase contrast microscopic images and (C) Quantifications of senescence-associated β-galactosidase staining in DFUFs and NFFs. $*p < 0.05$. Scale bar 100 μm.

both DFUF and NFF cell lines at passage 7 and found a 2.5-fold increase in the number of SA-β-gal positive cells in DFUFs as compared to NFFs ($p = 0.04$). Hence, we conclude that genomic data functionally correlate with induced senescence in DFUFs.

DISCUSSION

Emerging evidence suggests that dysregulated expression of miRNAs has substantial influences on cellular transcriptome, and eventually leads to impaired cellular functions in skin diseases.[9–11] In this study, we utilized an integrative miRNA–mRNA array analysis to identify potential miRNA mediated regulatory mechanisms in DFU-derived primary dermal fibroblasts that may contribute to the development of DFUs. Using this approach, we identified 331 reciprocal pairs of miRNA–mRNA that were differentially expressed between DFUFs and NFFs. We focused our study on the changes in DFUF transcriptome regulated by 43 induced miRNAs (including miR-21-5p, miR-34a-5p, miR-143-3p, and miR-145-5p cluster) that lead to impaired fibroblast functions, such as reduced cell migration and proliferation, induced cell differentiation and senescence, which represent key processes by which dermal fibroblasts support normal wound healing.

Several identified miRNAs and their target genes contribute to tissue fibrosis, which is one of histopathologic characteristics associated with DFUs.[23] Up-regulation of miR-21-5p has been observed in dermal compartment of chronic wounds and skin diseases, including in primary dermal fibroblasts derived from VLUs[11] and systemic sclerosis,[24] as well as in normal dermal fibroblasts that undergo replicative and stress-induced senescence stage.[25] Consistent with these observations, we found a significant increase of miR-21-5p expression in DFUF, and corresponding down-regulation of its five target genes, namely integrin associated protein (CD47), S100 calcium binding protein A10 (S100A10), protein sprouty homolog 1

(SPRY1), signal transducer and activator of transcription 3 (STAT3), reversion-inducing-cysteine-rich protein with kazal motifs (RECK). It has been reported that miR-21-5p suppresses RECK and SPRY1 expression by direct targeting 3′-UTR.[15,19] RECK is a membrane-anchored glycoprotein, which negatively regulates MMPs[26,27] and modulate cell-ECM interaction.[28] SPRY1 is a potent inhibitor of the Ras/MEK/ERK pathway.[29] Down-regulation of SPRY1 by hypoxia-mediated miR-21 induction leads to hypoxia-induced cell death and cell-cycle arrest.[17] Moreover, miR-21-mediated SPRY1 down-regulation has been linked to interstitial fibrosis in various organs.[19,29,30] Therefore, miR-21 induction may also lead to development of fibrosis. In addition to miR-21, miR-145 has been shown to regulate fibroblast differentiation and myofibroblast functions in the pathogenesis of fibrosis of multiple organs.[9,13,31,32] TGF-β1 has been shown to induce expression miR-145/-143 cluster, which in turn inhibits Kruppel-Like Factor 4 (KLF4), a known inhibitor of α-SMA, hence up-regulating α-SMA expression and functions of skin myofibroblasts.[33] In this study, we showed both induced expression of miR-145 and, as a consequence, up-regulation of α-SMA expression in DFUFs. Since myofibroblasts facilitate wound contraction, specifically in granulation tissue during acute wound healing, it is tempting to speculate that the up-regulation of miR-145-5p contributes to the deregulation of fibroblast differentiation. Providing that the appropriate execution of the wound healing process is dependent on temporal cellular functions, deregulation of fibroblast differentiation and increased myofiroblast population at the wrong time may be detrimental to healing. The specific role of miR-145 in enrichment of myofibroblast population in DFUs remains to be further elucidated. Collectively, induction of both miR-21-5p and miR-145 found in DFUFs may contribute to myofibroblast differentiation and tissue fibrosis found in DFUs.

In addition to fibrosis, changes in cellular migration and proliferation were also found in DFUs and confirmed in cellular assays using DFUFs. The changes in these cellular functions correspond to induction of several miRNAs, including miR-21 and miR-145. Predicted downstream targets miR-21-5p S100A10, STAT3, and CD47, are intensively involved in regulation of cell migration and proliferation. Down-regulation of S100A10 decreases migration and proliferation of A549 cells via the interaction with DLC1.[34] Embryonic fibroblasts derived from STAT3-null mice display migratory deficiency[35] and blockade of STAT3 expression decreases renal fibroblast proliferation.[36] Furthermore, inhibition of active CD47 decreases cellular migration.[37] Another miRNA that, together with miR-21-5p, may contribute to deregulation of migration and proliferation is miR-145. It is known as a tumor suppressor frequently reduced in cancers, displaying inhibitory effects in cell proliferation and migration.[38–40] Indeed, multiple target genes of miR-145 we identified in DFUFs regulate cell migration and proliferation. miR-145 was shown to suppress cell growth by down-regulating insulin receptor substrate-1 (IRS-1), one of the key molecules in insulin-like growth factor (IGF)-I and insulin mediated intracellular signaling.[41] miR-145 is also known to targets platelet derived growth factor D (PDGFD), which acts as fibroblast mitogen/chemoattractant and stimulates choroidal fibroblast proliferation, survival and migration.[42] Taken together, induction of miR-145-5p found in DFUFs, is shown to be a potent regulator of multiple fibroblast functions, including cell proliferation, migration and myofibroblast differentiation, all of which have been confirmed in cellular assays. In addition, induction of miR-21 in DFUFs may also contribute to delayed cellular proliferation and migration and induction of senescence.

Although up-regulation of miR-34a has been detected in the serum of type 2 diabetes patients,[43] we have previously shown that its expression remains unchanged in diabetic fibroblasts derived from intact foot skin,[13] suggesting the induction miR-34a found in DFUF is associated with ulceration, rather than with diabetes. Interestingly, miR-34a has been reported linked to fibroblast senescence.[44,45] Up-regulation of miR-34a is observed in both irreversible proliferative arrest of replicative senescence and hydrogen peroxide-induced premature senescence.[44,45] It shifts proliferating cells to senescence via either or both p53/p21 and p16/pRb pathways.[46] Moreover, in another type of chronic nonhealing wound, VLUs, characteristics associated with senescent cells have been observed in fibroblasts derived from wound edge.[47] In consistency, down-regulation of GAS1 was also observed in DFUF profile. Although the specific regulatory pathways that are driving DFU fibroblast to senescence stage remain to be determined, it is highly possible that miR-34a contribute to this process.

Altered miRNA and gene expression profiles of DFUFs may be associated with different fibroblast lineages. However, very little is known regarding miRNA-mediated regulation of distinct linages. Our data may indicate that inhibited proliferation and activated differentiation is consistent with characteristics of reticular fibroblasts.[48–50] However, there is no distinctive lineage phenotype that emerged in our analyses and further studies are needed to better characterize DFUF population.

Our previous study showed that diabetic foot fibroblasts have very similar miRNA and mRNA profiles compared to NFFs,[13] and deregulated miRNA–mRNA pairings we identified here are specific in DFUFs. Therefore, it is reasonable to conclude that altered miRNA expression coupled with impaired cellular functions are associated with ulceration, but not an outcome of pathologic process diabetes. In summary, our findings suggest that aberrant expression of three miRNAs (miR-21-5p, miR-34a-5p and miR-145-5p) lead to deregulation of DFU derived fibroblasts and cellular functions indispensable for successful wound healing: proliferation, migration, differentiation, and senescence.

ACKNOWLEDGMENTS

We thank all members of the Tomic-Canic, Garlic and Veves laboratories for their help and support. We are very grateful to the Clinical Research Wound Healing Program (Carol Kittles, Aliette Espinosa, Dr. Alejandra Vivas, Dr. Katherine Barquerizo-Nole) for their assistance with patients and collection of specimens. We also thank Dr. Antonio Barrientos for generously sharing laboratory resources and equipment and we acknowledge the use of University of Miami Genomic Facility.

Source of Funding: This work was funded by NIH grants DK098055 (JG), NR013881 (MT-C), University of Miami

SAC Award SAC 2013-19 (MT-C), and the UMSDRC of the Department of Dermatology and Cutaneous Surgery at the University of Miami Miller School of Medicine.

Conflict of Interest: The authors have no conflict of interest.

REFERENCES

1. Boulton AJ, Vileikyte L, Ragnarson-Tennvall G, Apelqvist J. The global burden of diabetic foot disease. *Lancet* 2005; 366: 1719–24.
2. Brem H, Tomic-Canic M. Cellular and molecular basis of wound healing in diabetes. *J Clin Invest* 2007; 117: 1219–22.
3. Jeffcoate WJ, Harding KG. Diabetic foot ulcers. *Lancet* 2003; 361: 1545–51.
4. Falanga V. Wound healing and its impairment in the diabetic foot. *Lancet* 2005; 366: 1736–43.
5. Brem H, Golinko MS, Stojadinovic O, Kodra A, Diegelmann RF, Vukelic S, et al. Primary cultured fibroblasts derived from patients with chronic wounds: a methodology to produce human cell lines and test putative growth factor therapy such as GMCSF. *J Transl Med* 2008; 6: 75.
6. Maione AG, Brudno Y, Stojadinovic O, Park LK, Smith A, Tellechea A, et al. Three-dimensional human tissue models that incorporate diabetic foot ulcer-derived fibroblasts mimic in vivo features of chronic wounds. *Tissue Eng Part C Methods* 2015; 21: 499–508.
7. Park LK, Maione AG, Smith A, Gerami-Naini B, Iyer LK, Mooney DJ, et al. Genome-wide DNA methylation analysis identifies a metabolic memory profile in patient-derived diabetic foot ulcer fibroblasts. *Epigenetics* 2014; 9: 1339–49.
8. Ambros V. The functions of animal microRNAs. *Nature* 2004; 431: 350–5.
9. Gras C, Ratuszny D, Hadamitzky C, Zhang H, Blasczyk R, Figueiredo C. miR-145 contributes to hypertrophic scarring of the skin by inducing myofibroblast activity. *Mol Med* 2015; 21: 296–304.
10. Huang RY, Li L, Wang MJ, Chen XM, Huang QC, Lu CJ. An exploration of the role of microRNAs in psoriasis: a systematic review of the literature. *Medicine* 2015; 94: e2030.
11. Pastar I, Khan AA, Stojadinovic O, Lebrun EA, Medina MC, Brem H, et al. Induction of specific microRNAs inhibits cutaneous wound healing. *J Biol Chem* 2012; 287: 29324–35.
12. Deppe J, Steinritz D, Santovito D, Egea V, Schmidt A, Weber C, et al. Upregulation of miR-203 and miR-210 affect growth and differentiation of keratinocytes after exposure to sulfur mustard in normoxia and hypoxia. *Toxicol Lett* 2016; 244: 81–7.
13. Ramirez HA, Liang L, Pastar I, Rosa AM, Stojadinovic O, Zwick TG, et al. Comparative genomic, microRNA, and tissue analyses reveal subtle differences between non-diabetic and diabetic foot skin. *PLoS One* 2015; 10: e0137133.
14. Vukelic S, Stojadinovic O, Pastar I, Vouthounis C, Krzyzanowska A, Das S, et al. Farnesyl pyrophosphate inhibits epithelialization and wound healing through the glucocorticoid receptor. *J Biol Chem* 2010; 285: 1980–8.
15. Hu SJ, Ren G, Liu JL, Zhao ZA, Yu YS, Su RW, et al. MicroRNA expression and regulation in mouse uterus during embryo implantation. *J Biol Chem* 2008; 283: 23473–84.
16. Junker A, Krumbholz M, Eisele S, Mohan H, Augstein F, Bittner R, et al. MicroRNA profiling of multiple sclerosis lesions identifies modulators of the regulatory protein CD47. *Brain* 2009;132 (Pt 12): 3342–52.
17. Polytarchou C, Iliopoulos D, Hatziapostolou M, Kottakis F, Maroulakou I, Struhl K, et al. Akt2 regulates all Akt isoforms and promotes resistance to hypoxia through induction of miR-21 upon oxygen deprivation. *Cancer Res* 2011; 71: 4720–31.
18. Shi B, Sepp-Lorenzino L, Prisco M, Linsley P, deAngelis T, Baserga R. Micro RNA 145 targets the insulin receptor substrate-1 and inhibits the growth of colon cancer cells. *J Biol Chem* 2007; 282: 32582–90.
19. Thum T, Gross C, Fiedler J, Fischer T, Kissler S, Bussen M, et al. MicroRNA-21 contributes to myocardial disease by stimulating MAP kinase signalling in fibroblasts. *Nature* 2008; 456: 980–4.
20. Liu R, Liao J, Yang M, Sheng J, Yang H, Wang Y, et al. The cluster of miR-143 and miR-145 affects the risk for esophageal squamous cell carcinoma through co-regulating fascin homolog 1. *PLoS One* 2012; 7: e33987.
21. Kent OA, McCall MN, Cornish TC, Halushka MK. Lessons from miR-143/145: the importance of cell-type localization of miRNAs. *Nucleic Acids Res* 2014; 42: 7528–38.
22. Debacq-Chainiaux F, Pascal T, Boilan E, Bastin C, Bauwens E, Toussaint O. Screening of senescence-associated genes with specific DNA array reveals the role of IGFBP-3 in premature senescence of human diploid fibroblasts. *Free Radic Biol Med* 2008; 44: 1817–32.
23. Cecilia-Matilla A, Lazaro-Martinez JL, Aragon-Sanchez J, Garcia-Morales E, Garcia-Alvarez Y, Beneit-Montesinos JV. Histopathologic characteristics of bone infection complicating foot ulcers in diabetic patients. *J Am Podiatr Med Assoc* 2013; 103: 24–31.
24. Zhu H, Li Y, Qu S, Luo H, Zhou Y, Wang Y, et al. MicroRNA expression abnormalities in limited cutaneous scleroderma and diffuse cutaneous scleroderma. *J Clin Immunol* 2012; 32: 514–22.
25. Dellago H, Preschitz-Kammerhofer B, Terlecki-Zaniewicz L, Schreiner C, Fortschegger K, Chang MW, et al. High levels of oncomiR-21 contribute to the senescence-induced growth arrest in normal human cells and its knock-down increases the replicative lifespan. *Aging Cell* 2013; 12: 446–58.
26. Oh J, Takahashi R, Kondo S, Mizoguchi A, Adachi E, Sasahara RM, et al. The membrane-anchored MMP inhibitor RECK is a key regulator of extracellular matrix integrity and angiogenesis. *Cell* 2001; 107: 789–800.
27. Omura A, Matsuzaki T, Mio K, Ogura T, Yamamoto M, Fujita A, et al. RECK forms cowbell-shaped dimers and inhibits matrix metalloproteinase-catalyzed cleavage of fibronectin. *J Biol Chem* 2009; 284: 3461–9.
28. Kimura T, Okada A, Yatabe T, Okubo M, Toyama Y, Noda M, et al. RECK is up-regulated and involved in chondrocyte cloning in human osteoarthritic cartilage. *Am J Pathol* 2010; 176: 2858–67.
29. Adam O, Lohfelm B, Thum T, Gupta SK, Puhl SL, Schafers HJ, et al. Role of miR-21 in the pathogenesis of atrial fibrosis. *Basic Res Cardiol* 2012; 107: 278.
30. Zanotti S, Gibertini S, Curcio M, Savadori P, Pasanisi B, Morandi L, et al. Opposing roles of miR-21 and miR-29 in the progression of fibrosis in Duchenne muscular dystrophy. *Biochim Biophys Acta* 2015; 1852: 1451–64.
31. Wang YS, Li SH, Guo J, Mihic A, Wu J, Sun L, et al. Role of miR-145 in cardiac myofibroblast differentiation. *J Mol Cell Cardiol* 2014; 66: 94–105.
32. Yang S, Cui H, Xie N, Icyuz M, Banerjee S, Antony VB, et al. miR-145 regulates myofibroblast differentiation and lung fibrosis. *FASEB J* 2013; 27: 2382–91.

33. Davis-Dusenbery BN, Chan MC, Reno KE, Weisman AS, Layne MD, Lagna G, et al. Down-regulation of Kruppel-like factor-4 (KLF4) by microRNA-143/145 is critical for modulation of vascular smooth muscle cell phenotype by transforming growth factor-beta and bone morphogenetic protein 4. *J Biol Chem* 2011; 286: 28097–110.
34. Yang X, Popescu NC, Zimonjic DB. DLC1 interaction with S100A10 mediates inhibition of in vitro cell invasion and tumorigenicity of lung cancer cells through a RhoGAP-independent mechanism. *Cancer Res* 2011; 71: 2916–25.
35. Ng DC, Lin BH, Lim CP, Huang G, Zhang T, Poli V, et al. Stat3 regulates microtubules by antagonizing the depolymerization activity of stathmin. *J Cell Biol* 2006; 172: 245–57.
36. Pang M, Ma L, Liu N, Ponnusamy M, Zhao TC, Yan H, et al. Histone deacetylase 1/2 mediates proliferation of renal interstitial fibroblasts and expression of cell cycle proteins. *J Cell Biochem* 2011; 112: 2138–48.
37. Zhang Y, Sime W, Juhas M, Sjolander A. Crosstalk between colon cancer cells and macrophages via inflammatory mediators and CD47 promotes tumour cell migration. *Eur J Cancer* 2013; 49: 3320–34.
38. Zheng M, Sun X, Li Y, Zuo W. MicroRNA-145 inhibits growth and migration of breast cancer cells through targeting oncoprotein ROCK1. *Tumour Biol* 2016; 37: 8189–96.
39. Cho WC, Chow AS, Au JS. Restoration of tumour suppressor hsa-miR-145 inhibits cancer cell growth in lung adenocarcinoma patients with epidermal growth factor receptor mutation. *Eur J Cancer* 2009; 45: 2197–206.
40. Wang Z, Zhang X, Yang Z, Du H, Wu Z, Gong J, et al. MiR-145 regulates PAK4 via the MAPK pathway and exhibits an antitumor effect in human colon cells. *Biochem Biophys Res Commun* 2012; 427: 444–9.
41. Wang Y, Hu C, Cheng J, Chen B, Ke Q, Lv Z, et al. MicroRNA-145 suppresses hepatocellular carcinoma by targeting IRS1 and its downstream Akt signaling. *Biochem Biophys Res Commun* 2014; 446: 1255–60.
42. Kumar A, Hou X, Lee C, Li Y, Maminishkis A, Tang Z, et al. Platelet-derived growth factor-DD targeting arrests pathological angiogenesis by modulating glycogen synthase kinase-3beta phosphorylation. *J Biol Chem* 2010; 285: 15500–10.
43. Kong L, Zhu J, Han W, Jiang X, Xu M, Zhao Y, et al. Significance of serum microRNAs in pre-diabetes and newly diagnosed type 2 diabetes: a clinical study. *Acta Diabetol* 2011; 48: 61–9.
44. Maes OC, Sarojini H, Wang E. Stepwise up-regulation of microRNA expression levels from replicating to reversible and irreversible growth arrest states in WI-38 human fibroblasts. *J Cell Physiol* 2009; 221: 109–19.
45. Khee SG, Yusof YA, Makpol S. Expression of senescence-associated microRNAs and target genes in cellular aging and modulation by tocotrienol-rich fraction. *Oxid Med Cell Longev* 2014; 2014: 725929.
46. Liu FJ, Wen T, Liu L. MicroRNAs as a novel cellular senescence regulator. *Ageing Res Rev* 2012; 11: 41–50.
47. Mendez MV, Stanley A, Park HY, Shon K, Phillips T, Menzoian JO. Fibroblasts cultured from venous ulcers display cellular characteristics of senescence. *J Vasc Surg* 1998; 28: 876–83.
48. Sorrell JM, Baber MA, Caplan AI. Construction of a bilayered dermal equivalent containing human papillary and reticular dermal fibroblasts: use of fluorescent vital dyes. *Tissue Eng* 1996; 2: 39–49.
49. Sorrell JM, Baber MA, Caplan AI. Site-matched papillary and reticular human dermal fibroblasts differ in their release of specific growth factors/cytokines and in their interaction with keratinocytes. *J Cell Physiol* 2004; 200: 134–45.
50. Harper RA, Grove G. Human skin fibroblasts derived from papillary and reticular dermis: differences in growth potential in vitro. *Science* 1979; 204: 526–7.

Supporting Information

Additional Supporting Information may be found in the online version of this article.